Materials Advances

ROYAL SOCIETY OF CHEMISTRY

PAPER

View Article Online
View Journal | View Issue

Cite this: *Mater. Adv.*, 2021, 2, 3993

Preparation of polymers possessing dynamic N-hindered amide bonds through ketene-based chemistry for repairable anticorrosion coatings

Tsai-Wei Chuo, Jyun-Ting Hou and Ying-Ling Liu *

Received 16th April 2021,
Accepted 2nd May 2021

DOI: 10.1039/d1ma00349f

rsc.li/materials-advances

Dynamic covalent bonds, particularly the ones exhibiting bond-breaking and bond-regeneration under ambient conditions, are attractive for the design and application of smart materials. This study demonstrates that the Meldrum's acid-based ketene chemistry is an effective approach to build up dynamic N-hindered amide bonds effectively workable at ambient conditions and under sunlight. The corresponding polyamides have been applied for sunlight-driven and self-repairing polymeric materials, and anticorrosion coatings. In addition to exhibiting sunlight-driven and self-repairing features on scratched surfaces, a high anticorrosion recovery of about 97% has been recorded. A smart anticorrosion coating requiring less maintenance is demonstrated.

Introduction

Dynamic covalent bonds could effectively build up reversibly-crosslinked polymers with repairable features.[1–7] When polymeric materials are cut or damaged, the mechanism responsible for the repairing features majorly involve 3 steps: (1) breaking the crosslinked polymer networks *via* the dissociation of the dynamic bonds, (2) chain motion to heal/repair the crosslinked polymers in bulk and exterior aspect, and (3) reestablishment of the crosslinked networks at the damaged region through the reformation of the dynamic bonds. As the first step plays the critical role in triggering the repairing process, the conditions required for the dissociation of the dynamic bonds become the critical and necessary presupposition for the repairable polymers. Taking the most studied Diels–Alder (DA) adduct-based repairable polymers as examples,[7] the first step to activate the repairing process is the retro-DA reaction to break the DA adducts. As high temperatures are usually required to carry out the retro-DA reaction, self-repairing the DA adduct-based polymers could only be achieved at high temperatures. These materials lack intrinsic self-healing property. Another attractive trigger factor for the repairable polymers is ultraviolet (UV) irradiation.[8–12] Although repairable polymers responsive to UV irradiation have been widely reported, their repairing performance under sunlight treatment was not reported due to their poor responsive efficiency towards sunlight.[8–12]

Department of Chemical Engineering, National Tsing Hua University, 300044 Hsinchu, Taiwan. E-mail: liuyl@mx.nthu.edu.tw; Fax: +886-3-5715408; Tel: +886-3-5711450

Repairable polymers, being effectively workable under sunlight irradiation and/or at around ambient conditions, are attractive to integrate the autonomous and intrinsic self-healing features in the polymers. The repairing action could be achieved under a natural environment without additional stimuli and trigger factors. Self-healing polymers under an ambient environment, which employ dynamic-covalent diarylbibenzofuranone bonds[13,14] and boronic esters,[15,16] have been reported. On the other hand, the sensitivity of the dynamic covalent bonds towards sunlight irradiation could be enhanced by decreasing the bond strengths of the UV-responsive linkages. One approach is the introduction of an electron-donating group, which could effectively lower the disulfide bond dissociation energy. One example is the disulfide-bond-based sunlight-driven self-healing polymers.[17] Similar strategies have been applied to thermal-responsive dynamic bonds. The incorporation of bulky substituents to urea bonds could significantly lower the bond dissociation energy of the hindered urea linkage, consequently making the urea bond dynamic and suitable for building up reversible and self-healing polymers.[18,19] Although sterically hindered amide bonds also exhibit similar features,[20] the preparation and application of dynamic-hindered amide bonds is somewhat restricted.[21] Unlike hindered urea linkages, which could be formed with a hindered amine and an isocyanate groups,[18] the formation of hindered amide bonds employs highly reactive ketene groups reacting with a hindered amine. Due to the high reactivity and poorly-controlled characteristic of the ketene groups, the developments of dynamic amide bond-based polymers are critically limited.

Meldrum's acid (MA) groups could convert to ketene groups *via* a thermolysis reaction with the evolution of CO_2 and acetone.[22] The MA-mediated ketene chemistry provides an

effective and controllable approach of employing ketene groups in polymer synthesis and functionalization.[23–26] In this study, we explored the first example of self-repairing polymers based on the dynamic N-hindered amide linkages through the MA-mediated ketene chemistry. The polyamides show sunlight-driven self-repairing property and are effective additives for introducing self-repairing features to anticorrosion coatings. The resulting coating shows a 97% recovery of anticorrosion efficiency under sunlight and ambient environment.

Results and discussion

A polysiloxane possessing pendant MA groups (PDMS-MA), reported in our previous study,[27] was utilized as the raw material in this study to build up self-healing polymers possessing dynamic amide bonds. Two secondary amines with bulky substituents (diamine I and diamine II) are used as the reactive precursors to react with the ketene groups generated from the MA thermolysis to result in N-hindered amide groups (Scheme 1). A crosslinked PDMS possessing dynamic amide bonds is obtained. The chain flexibility of PDMS-MA warrants the mobility of the polymer chains in the self-repairing process under an ambient condition. Through the MA thermolysis and ketene–amine addition reactions, PDMS-MA is crosslinked with the amine compounds to give the samples of CR-PAm-I and CR-PAm-II. In the case where the hindered amines are not added, PDMS-MA could perform a thermally-induced self-crosslinking reaction through the ketene dimerization reaction, resulting in the corresponding sample of CR-PDMS.[27] CR-PDMS does not possess the dynamic amide bonds and is used as a control sample for comparison in this study.

The 3 crosslinked samples were cut using a knife. The cut samples were applied to self-repairing tests (Fig. 1). The cut CR-PDMS sample did not demonstrate any repairing ability under the operation condition (80 °C for 24 h). In contrast, the cut pieces of CR-PAm-I and CR-PAm-II could recombine together to exhibit efficient self-repairing features. CR-PAm-I demonstrates a better self-repairing ability compared to CR-PAm-II, although CR-PAm-II has bulky substituents attached to the dynamic amide linkages. This result might be attributed to the relatively high electron-donating ability of the *t*-butyl groups of CR-PAm-II, compared to the i-propyl groups of CR-PAm-I. The electron-donating effects would strengthen the C–N bonds of the amide linkages of CR-PAm-II. The self-repairing tests on CR-PAm-I have been carried out under numerous conditions. The relatively high self-repairing efficiency was found at 80 °C due to the relatively high mobility of the decrosslinked polymer chains at high temperatures. Moreover, the self-repairing ability of CR-PAm-I under ambient conditions (under sunlight at daytime and at room temperature (about 25 °C) at night) is noteworthy. The sunlight-driven self-repairing ability of CR-PAm-I is further examined with an Instron (Fig. 2). The sunlight-driven repaired sample shows a strength of about 0.028 MPa, which is about 31% of the value recorded on the original sample. Since the CR-PAm-I sample was fully cut into 2 pieces, which were then recombined into one piece at a simple contact mode under the self-repairing condition, the resistance to the applied stress of the repaired sample is high enough to support the self-repairing ability.

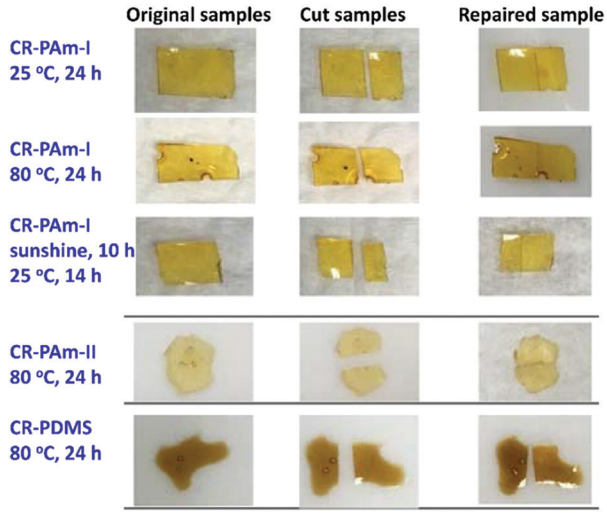

Fig. 1 Photographs showing the self-repairing tests on the crosslinked polyamide samples under different conditions. The tests on the crosslinked PDMS is included for a comparison.

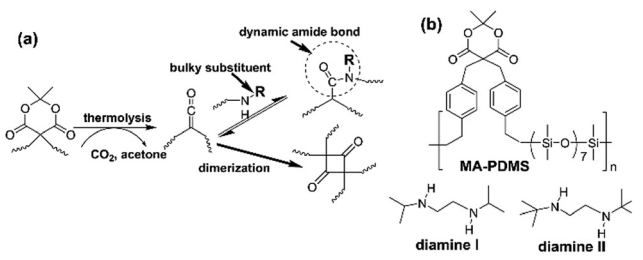

Scheme 1 (a) Thermolysis reaction of the Meldrum's acid group and the following ketene-based reactions to generate dynamic N-hindered amide bonds; (b) chemical structures of the agents used in this study for building up self-repairing polymers possessing dynamic N-hindered amide bonds.

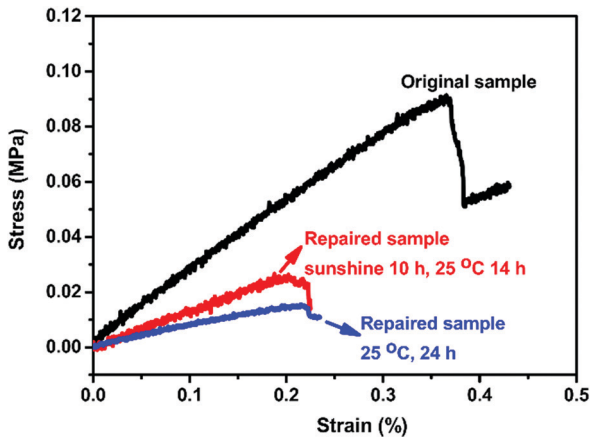

Fig. 2 Stress–strain curves of CR-PAm-I samples in self-repairing tests. The original sample was cut into 2 pieces and then merged again under the repairing conditions shown in the plot.

As the repaired sample obtained at 25 °C for 24 h (without sunlight treatment) only shows a strength of about 0.011 MPa, the sunlight treatment brings a positive effect on the promotion of the self-repairing efficiency of the CR-PAm-I sample. The sunlight-driven and self-repairing ability of CR-PAm-I is demonstrated. CR-PAm-I could be the first example of sunlight-driven and self-repairing polyamides since most reported cases are disulfide-based polymers.[17,29,30]

The reversible reaction of the hindered amide groups, from the reaction between a secondary amine with bulky substituents and a ketene group, has been examined with a model reaction between a methylated MA compound (MAM) and diamine I. The reaction has been traced *via* NMR (Fig. 3). After being heated at 140 °C for 3 min, the occurrence of the MA thermolysis reaction is characterized by the evolution of acetone[22] showing the resonance peak at δ = 2.16 ppm and the C$\underline{H}_3$-ketene group at δ = 1.21 ppm. The reaction of diamine I and the ketene group forms the corresponding hindered amide groups, showing resonance peaks at δ = 1.41 ppm ((C$\underline{H}_3$)$_2$CH–N), δ = 3.05 ppm (–C$\underline{H}_2$–N–C(=O)), and δ = 3.42 ppm ((CH$_3$)$_2$C$\underline{H}$–N). The obtained amide sample was then heated at 45 °C. In the corresponding ^{1}H NMR spectrum, the intensities of the resonance peaks associated with the hindered amide groups (δ = 3.05 ppm and δ = 3.42) decrease significantly. The increase in the intensities of peaks at δ = 1.07 ppm, δ = 2.55 ppm, and δ = 2.66 ppm indicates the regeneration of the isopropyl group-substituted secondary amine. The interchange reaction between the amide and amine groups has been further examined with ^{13}C NMR. The amide group (C(=O)–N) exhibits a resonance peak at about δ = 167 ppm. This peak disappears for the sample being heated at 45 °C, indicating the occurrence of the scissoring reaction of amide bonds.

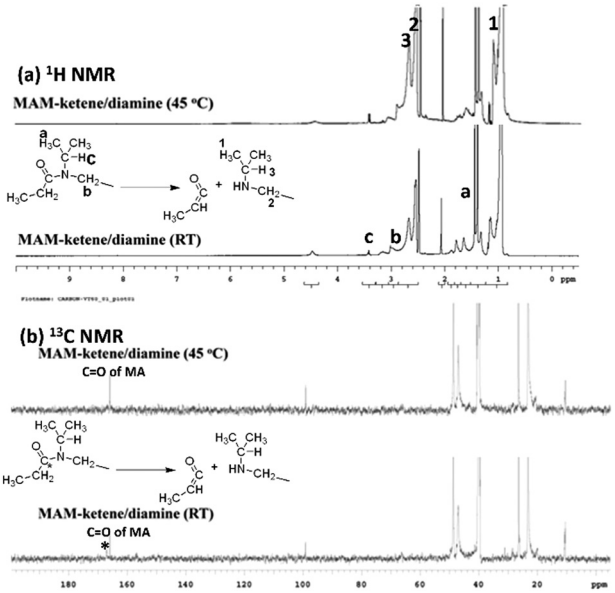

Fig. 3 (a) ^{1}H NMR and (b) ^{13}C NMR spectra of the reaction product of MAM and diamine I at room temperature and under heating at 45 °C. The changes in the spectra support the dissociation of the hindered amine bonds.

The reversible feature of the above-mentioned reaction has also been examined through tracing the reaction between PDMS-MA and diamine I *via* FTIR spectroscopy (Fig. 4). PDMS-MA was heated at 270 °C for 5 min to demonstrate the formation of ketene groups at 2100 cm^{-1}.[22] After being mixed with diamine I, the peak intensity of ketene groups decreases gradually. Moroever, the amide absorption peak at 1650 cm^{-1} is observed. The changes in the amide group absorption with the increase in temperature have been recorded. The absorption intensity of the hindered amide groups decreases and that of the secondary amine absorption increases significantly in the spectra recorded at about 35 to 45 °C, indicating the occurrence of the amide bond dissociation reaction. The amide absorption regains its intensity while the sample is being cooled to low temperatures (about 20 °C). The absorption intensity decreases again in the second heating run. The results support the reversibility of the amide bond dissociation and reformation in the heating–cooling processes.

The results discussed above support to (i) MA-possessing polymers are potential precursors for the preparation of cross-linked polymers possessing dynamic amide bonds and (ii) the corresponding dynamic amide are effective for building up self-repairing polymers workable under ambient conditions. One of the potential applications of the as-prepared material has been examined as sunlight-driven and self-repairing car paint.[28] A commercial product of scratch-repairing car paint is utilized as the matrix with various amounts of CR-PAm-I.[31] The self-repairing car paint samples are coded as SR_CP-X, where X denotes the weight fraction of CR-PAm-I of the sample. SR_CP-X samples have been coated on cold-rolled stainless steel (CRS) pieces for self-repairing and anticorrosion tests. The sample surfaces were cut with a knife and then applied to 2 different self-repairing processes. One is at 25 °C for 24 h without being exposed to sunlight, and the other is under sunlight (outdoor temperature is about 25–30 °C) for 10 h and then at 25 °C in dark for another 14 h. The results are collected in Fig. 5. The pristine car paint does not exhibit self-repairing property under both treatment conditions, as there are no obvious changes on the cut print after the treatment. For SR_CP-20 and SR_CP-40, the samples do not exhibit quick self-repairing feature at 25 °C for 24 h due to their low CR-PAm-I contents. Nevertheless, the samples under the sunlight

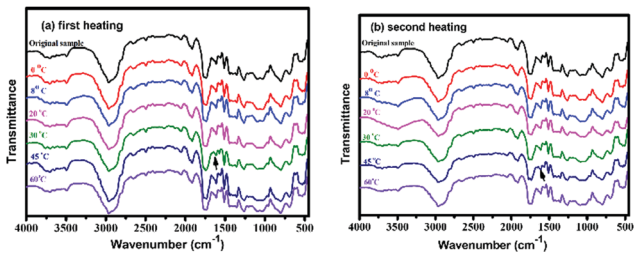

Fig. 4 FTIR spectra recorded for the CR-PAm-1 sample at various temperatures during a heating process: (a) the first heating run and (b) the second heating run. The black arrows pointing to the absorption peaks of the hindered amide groups.

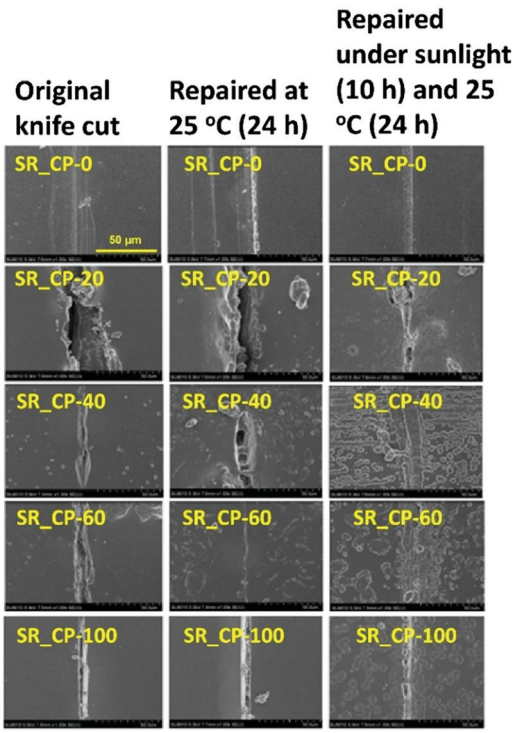

Fig. 5 SEM micrographs showing the self-repairing behaviors of the SR_CP-X samples (CR-PAm-I modified car paints).

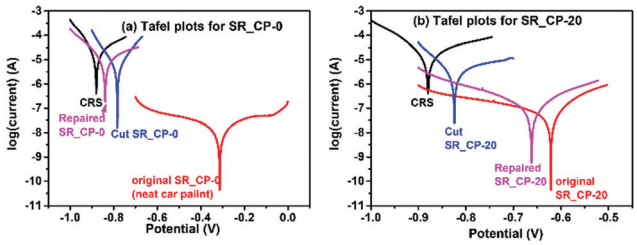

Fig. 6 Tafel plots of (a) neat SR_CP-0 (neat car paint) and (b) SR_CP-20 recorded in the self-repairing process.

Table 1 Anticorrosion recovery tests on the CR-Pam-I modified car paint-coated CRS samples

Sample	Corrosion rate (μm year^{-1})	Protection efficiency (%)	Resistance at 0.1 Hz (Ω)
Naked CRS	264	—	430
SR_CP-0	0.21	99.92	391 900
SR_CP-0, cut	54	79.28	948
SR_CP-0, repaired	13.7	47.92	670
SR_CP-20	1.0	99.60	117 700
SR_CP-20, cut	38	85.50	2588
SR_CP-20, repaired	2.0	99.24	31 460

treatment show certain extents of recovery of the cut prints. The sunlight treatment could enhance the self-repairing efficiency due to the increased temperatures of the samples under sunlight. The samples of SR_CP-60 exhibit a good self-repairing property. Nevertheless, the self-repairing performance of the pure CR-PAm-I sample (SR_CP-100) is not as high as SR_CP-60, particularly for the sample without sunlight treatment, due to the fact that the highly crosslinked structure of SR_CP-100 needs a relatively long time for chain motion and morphological repairing.

PAm-I has been used as an agent to impart self-repairing properties to a commercial product of car paint. The self-repairing property of the modified car paints (SR_CP-X samples coated on CRS pieces) have been evaluated with their anticorrosion performance with experimental data from both of the Tafel plots (corrosion rate (CR) and protection efficiency (PE)) and Bode plots.[32] The anticorrosion performance could be identified with the peak values of the current in Tafel plots (Fig. 6). The neat car paint has a high anticorrosion performance with a protection efficiency of about 99.92% (Table 1). The addition of CR-PAm-I to the car paint results in a slight decrease in the protection efficiency to 99.6% due to the fact that the structure design of CR-PAm-I is not mainly for the anticorroison aspect. In further studies, the incorporation of the electroactive feature[32] to CR-PAm-I might effectively address this issue. On the other hand, the neat car paint does not exhibit repairable features. Once some pinholes formed with the coating, corrosion might take place starting at the pinholes and then spread over the steel beneath the coating. Corrosion would take place readily even though the coating has a high protection efficiency. Since the neat car paint does not exhibit any self-repairing ability on the recovery of the anticorrosion property from the corresponding cut sample, the addition of CR-PAm-I to the car paint successfully introduces self-healing ability and anticorrosion recovery to the employed car paint. SR_CP-100 exhibits a certain anticorrosion ability with a CR of 4.7 μm year^{-1}, which is not as good as that of the neat car paint and could be attributed to the relatively poor adhesion strength towards the CRS surface. Although the self-healing efficiency increases with an increase in the dynamic amide bond contents, the anticorrosion efficiency would decrease with the increase in the CR-PAm-I contents. Hence, SR_CP-20 (with 20 wt% of CR-PAm-I) is the optimum sample with a balance between the self-healing ability and anticorrosion efficiency. The partial recovery of the anticorrosion properties of SR_CP-20 is noteworthy. From the data shown in Table 1, the neat car paint shows a high efficiency of anticorrosion with a CR of 0.21 μm year^{-1} (the CR value recorded on naked CRS: 264 μm year^{-1}) and a PE of 99.92%. The best result has been found with the SR_CP-20 sample. SR_CP-20 shows a CR and PE of 1.0 μm year^{-1} and 99.60%, respectively, indicating that an addition of 20 wt% of CR-PAm-I might slightly reduce the anticorrosion performance of the used car paint. Nevertheless, the anticorrosion efficiency of SR_CP-20 is still high for practical application. Moreover, applying a knife cut to the SR_CP-20-coated CRS sample significantly reduces its anticorrosion performance with an increase in the CR value to 38 μm year^{-1} and a reduced PE value of 85.5%. Unlike the neat car paint sample, the cut CR_CP-20 sample could be repaired under the treatment process mentioned above. After being repaired, a recovery of anticorrosion performance has been observed with a CR and PE of 2.0 μm year^{-1} and 99.24%, respectively. In terms of

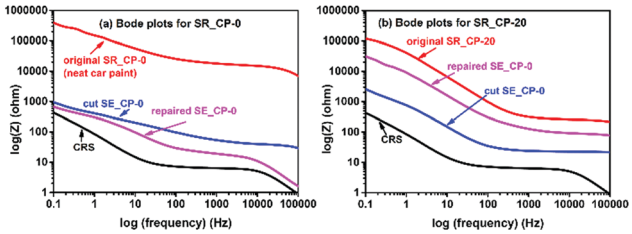

Fig. 7 Bode plots of (a) neat SR_CP-0 (neat car paint) and (b) SR_CP-20 recorded in the self-repairing process.

both CR and PE, a high anticorrosion performance recovery of about 97% is obtained. The results demonstrate the successful development of sunlight-driven self-repairing anticorrosion paints.

The anticorrosion properties of the as-prepared samples have also been evaluated *via* electrochemical impedance spectroscopy (EIS).[32] The resistance at low frequency (Z_o at 0.1 Hz) read from the Bode plots could be utilized as an index for the anticorrosion performance (Fig. 7). Compared to the Z_o value (430 Ω) of the naked CRS sample, the high Z_o value (391 900 Ω) of SR_CP-0 suggests the high anticorrosion performance of the pure car paint. The original car paint could not regain the anticorrosion property after being cut. On the other hand, although the Z_o value (117 700 Ω) of SR_CP-20 is not as high as the neat car paint, the addition of 20% of CR-PAm-I to the car paint could bring the self-repairing feature and anticorrosion recovery ability to the car paint, as a regain of the Z_o value from 2588 Ω to 31 460 Ω is observed. A sunlight-driven and self-repairing paint and anticorrosion coating needing very less maintenance has been demonstrated.

The surface temperatures of cars parked outdoor on a sunny day in April in Taiwan (atmosphere temperature: 31 °C at 13:00) have been recorded. The temperatures recorded on a white car and a black car are 47 °C and 70 °C, respectively. The temperatures are high enough to trigger the self-repairing processes of CR-PAm-I. It is concluded that the CR-PAm-I could perform its function of sunlight-driven repairable coating under ambient conditions.

Experimental

Materials

Meldrum's acid-functionalized polydimethylsiloxane (viscous liquid, PDMS-MA) was prepared in the laboratory according to the method reported in the previous publication.[27] *N*,*N*′-Diisopropylethylenediamine (diamine I, 97%) and *N*,*N*′-di-*t*-butylethylenediamine (diamine II, 98%) are purchased from Alfa Asear Chemical Co. and used as received. 2,2,5-Trimethyl-1,3-dioxane-4,6-dione (methylated Meldrum's acid, MAM, 97%) was received from Sigma-Aldrich Chemical Co.

Instrumental characterization

FTIR spectra were recorded on a PerkinElmer spectrum II FTIR spectrometer equipped with a temperature-controller of samples. The mixture of PDMS-MA and diamine I were coated on KBr pellet for measurements in the wavenumber range of 400 cm^{-1}–4000 cm^{-1}. SEM micrographs were recorded using a Hitachi SU8000 field-emission SEM.

Preparation of crosslinked polyamides (CR-PAm-I and CR-PAm-II). PDMS-MA was mixed with diamine I in stoichiometric amounts. The mixture was coated on a NaCl substrate (cell window for FTIR). The sample was heated at 240 °C for 5 min, quickly quenched to room temperature, and then reacted at 80 °C for 4 h to obtain CR-PAm-I. CR-PAm-II was obtained in the same manner using diamine II as the reactant.

Preparation of CR-PAm-I modified car paint. The mixtures and PDMS-MA and diamine I in stoichiometric ratio were added to the commercial product of scratch car paint in different amounts. The samples were coated on cold-rolled stainless steel (CRS) pieces and then heated at 240 °C for 5 min, quickly quenched to room temperature, and then left to stand at 80 °C for 4 h. The as-prepared samples were applied for both surface self-repairing observations *via* SEM and anticorrosion tests.

Electrochemical analysis for anticorrosion evaluation. An electrochemical station of VoltaLab-PST050 equipped with a saturated calomel electrode (SCE) and a carbon rod counter electrode was utilized for the cyclic voltammetry measurements in the voltage range from −1.1 V to 0 V at a scan rate of 100 mV min^{-1}. A 3.5 wt% $NaCl_{(aq)}$ was used as the corrosive medium. The corrosion potential (E_{corr}) and corrosion current (I_{corr}) were determined *via* the Tafel extrapolation method.[32] The open circuit potential (OCP) *vs.* SCE at the equilibrium state was recorded as E_{corr}. Measurements were taken in the potential range from 500 mV below to 500 mV above the E_{corr} at a scan rate of 100 mV min^{-1}. I_{corr} was read from the extrapolation of the obtained Tafel plot and was applied to the calculation of the corresponding corrosion rate (CR)[33] and protection efficiency (PE).[34]

$$\text{CR (mm year}^{-1}) = (0.13 \times I_{corr} \times (\text{equivalent wt of CRS}))/((\text{area of CRS}) \times (\text{density of CRS})) \quad (1)$$

$$\text{PE (\%)} = (I_{corr} - I_{corr}(\text{CRS}))/I_{corr} \times 100\% \quad (2)$$

A Metrohm Autolab FRA2 electrochemical impedance spectroscopy (EIS) instrument was employed for the EIS measurements. An SCE and a carbon rode were utilized as the reference electrode and the counter electrode, respectively. A 3.5 wt% $NaCl_{(aq)}$ was applied as the electrolyte.

Conclusions

Taking advantage of the Meldrum's acid mediated ketene chemistry, dynamic amide bonds have been employed in building up self-repairing polymers, which are workable at room temperature and under sunlight. The polyamides are effective additives to introduce self-repairing features to anticorrosion coating and painting. The products show high efficiency in sunlight-driven and self-repairing properties and recovery of anticorrosion performance. The reported smart

materials are highly attractive for a wide range of applications in terms of manpower- and energy-saving issues and sustainability.

Author contributions

T.-W. C.: investigation, methodology; J.-T. H.: investigation, formal analysis; Y.-L. L.: conceptualization, supervision, writing – original draft, writing – review and editing.

Conflicts of interest

There are no conflicts to declare.

Acknowledgements

The authors thank the Ministry of Science and Technology (MOST) of Taiwan for the financial supports on this work (Grant No. MOST 108-2221-E-007-015-MY3).

Notes and references

1 M. M. Perera and N. Ayres, Dynamic covalent bonds in self-healing, shape memory, and controllable stiffness hydrogels, *Polym. Chem.*, 2020, **11**, 1410–1423.
2 P. Chakma and D. Konkolewicz, Dynamic covalent bonds in polymeric materials, *Angew. Chem., Int. Ed.*, 2019, **58**, 9682–9695.
3 S. Nevejans, N. Ballard, M. Fernández, B. Reck, S. J. García and J. M. Asua, The challenges of obtaining mechanical strength in self-healing polymers containing dynamic covalent bonds, *Polymer*, 2019, **179**, 121670.
4 C. Kim and N. Yoshie, Polymers healed autonomously and with the assistance of ubiquitous stimuli: How can we combine mechanical strength and a healing ability in polymers?, *Polym. J.*, 2018, **50**, 919–929.
5 J. Dahlke, S. Zechel, M. D. Hager and U. S. Schubert, How to design a self-healing polymer: General concepts of dynamic covalent bonds and their application for intrinsic healable materials, *Adv. Mater. Interfaces*, 2018, **5**, 1800051.
6 Y. Jin, W. Wang, P. Tayton and W. Zhang, Dynamic covalent chemistry approaches toward macrocycles, molecular cages, and polymers, *Acc. Chem. Res.*, 2014, **47**, 1575–1586.
7 Y. L. Liu and C. W. Chuo, Self-healing polymers based on thermally reversible Diels–Alder chemistry, *Polym. Chem.*, 2013, **4**, 2194–2205.
8 Z. L. Pianowski, J. Karchera and K. Schneider, Photoresponsive self-healing supramolecular hydrogels for light-induced release of DNA and doxorubicin, *Chem. Commun.*, 2016, **52**, 3143–3146.
9 P. Froimowicz, H. Frey and K. Landfester, Towards the generation of self-healing materials by means of a reversible photo-induced approach, *Macromol. Rapid Commun.*, 2011, **32**, 468–473.
10 T. Manouras and M. Vamvakaki, Field responsive materials: Photo-, electro-, magnetic- and ultrasound-sensitive polymers, *Polym. Chem.*, 2017, **8**, 74–96.
11 Q. Zhang, D. H. Qu and H. Tian, Photo-regulated supramolecular polymers: Shining beyond disassembly and reassembly, *Adv. Opt. Mater.*, 2019, **7**, 1900033.
12 H. Liu, B. Xu, X. Yang, Z. Li, Z. Mo, Y. Yao and S. Lin, Ultraviolet and infrared two-wavelength modulated self-healing materials based on azobenzene-functionalized carbon nanotubes, *Compos. Commun.*, 2020, **19**, 233–238.
13 K. Imato, M. Nishihara, T. Kanehara, Y. Amamoto, A. Takahara and H. Otsuka, Self-healing of chemical gels cross-linked by diarylbibenzofuranone-based trigger-free dynamic covalent bonds at room temperature, *Angew. Chem., Int. Ed.*, 2012, **51**, 1138–1142.
14 K. Imato, A. Takahara and H. Otsuka, Self-healing of a cross-linked polymer with dynamic covalent linkages at mild temperature and evaluation at macroscopic and molecular levels, *Macromolecules*, 2015, **48**, 5632–5639.
15 J. J. Cash, T. Kubo, A. P. Bapat and B. S. Sumerlin, Room-temperature self-healing polymers based on dynamic-covalent boronic esters, *Macromolecules*, 2015, **48**, 2098–2106.
16 O. R. Cromwell, J. Chung and Z. Guan, Malleable and self-healing covalent polymer networks through tunable dynamic boronic ester bonds, *J. Am. Chem. Soc.*, 2015, **137**, 6492–6495.
17 D. J. Fortman, R. L. Snyder, D. T. Sheppard and W. R. Dichtel, Rapidly reprocessable cross-linked polyhydroxyurethanes based on disulfide exchange, *ACS Macro Lett.*, 2018, **7**, 1226–1231.
18 H. Ying, Y. Zhang and J. Cheng, Dynamic urea bond for the design of reversible and self-healing polymers, *Nat. Commun.*, 2014, **5**, 3218.
19 S. Zechel, R. Geitner, M. Abend, M. Siegmann, M. Enke, N. Kuhl, M. Klein, J. Vitz, S. Gräfe, B. Dietzek, M. Schmitt, J. Popp, U. S. Schubert and M. D. Hager, Intrinsic self-healing polymers with a high e-modulus based on dynamic reversible urea bonds, *NPG Asia Mater.*, 2017, **9**, e420.
20 M. Hutchby, C. E. Houlden, M. F. Haddow, S. N. G. Tyler, G. C. Lloyd-Jones and K. I. Booker-Milburn, Switching pathways: Room-temperature neutral solvolysis and substitution of amides, *Angew. Chem., Int. Ed.*, 2012, **51**, 548–551.
21 R. M. Lanigan, P. Starkov and T. D. Sheppard, Direct synthesis of amides from carboxylic acids and amines using $B(OCH_2CF_3)_3$, *J. Org. Chem.*, 2013, **78**, 4512–4523.
22 F. A. Leibfarth, M. Kang, M. Ham, J. Kim, L. M. Campos, N. Gupta, B. Moon and C. J. Hawker, A facile route to ketene-functionalized polymers for general materials applications, *Nat. Chem.*, 2010, **2**, 207–212.
23 Y. Miyamura, C. Park, K. Kinbara, F. A. Leibfarth, C. J. Hawker and T. Aida, ConCrolling volume shrinkage in soft lithography through heat-induced cross-linking of patterned nanofibers, *J. Am. Chem. Soc.*, 2011, **133**, 2840–2843.

24 J. Wu, S. T. Iacono, G. T. McCandless, G. W. Smith Jr. and B. M. Novak, Utilization of a Meldrum's acid towards functionalized fluoropolymers possessing dual reactivity for thermal crosslinking and post-polymerization modification, *Chem. Commun.*, 2015, **51**, 9220–9222.

25 L. K. Lin, C. C. Hu, W. C. Su and Y. L. Liu, Thermosetting resins with high fractions of free volume and inherently low dielectric constants, *Chem. Commun.*, 2015, **51**, 12760–12763.

26 Y. Chen, L. K. Lin, S. J. Chiang and Y. L. Liu, A cocatalytic effect between Meldrum's acid and benzoxazine compounds in preparation of high performance thermosetting resins, *Macromol. Rapid Commun.*, 2017, **38**, 1600616.

27 W. L. Su and Y. L. Liu, Self-crosslinkable and modifiable polysiloxanes possessing Meldrum's acid groups, *Polym. Chem.*, 2018, **9**, 4781–4788.

28 B. Ghosh and M. W. Urban, Self-repairing oxetane-substituted chitosan polyurethane networks, *Science*, 2009, **323**, 1458–1460.

29 W. M. Xu, M. Z. Rong and M. Q. Zhang, Sunlight driven self-healing, reshaping and recycling of a robust, transparent and yellowing resistant polymer, *J. Mater. Chem. A*, 2016, **4**, 10683–10690.

30 H. P. Xiang, M. Z. Rong and M. Q. Zhang, A facile method for imparting sunlight driven catalyst-free self-healability and recyclability to commercial silicone elastomer, *Polymer*, 2017, **108**, 339–347.

31 T. W. Chuo, T. C. Wei and Y. L. Liu, Electrically driven self-healing polymers based on reversible guest–host complexation of β-cyclodextrin and ferrocene, *J. Polym. Sci., Part A: Polym. Chem.*, 2013, **51**, 3395–3403.

32 T. W. Chuo and Y. L. Liu, Furan-functionalized aniline trimer based self-healing polymers exhibiting high efficiency of anticorrosion, *Polymer*, 2017, **125**, 227–233.

33 T. I. Yang, C. W. Peng, Y. L. Lin, C. J. Wang, G. Edgington, A. Mylonakis, T. C. Huang, C. H. Hsu, R. M. Yeh and Y. Wei, Synergistic effect of electroactivity and hydrophobicity on the anticorrosion property of room-temperature-cured epoxy coatings with multi-scale structures mimicking the surface of *Xanthosoma sagittifolium* leaf, *J. Mater. Chem.*, 2012, **22**, 15845–15852.

34 T. W. Chou, R. M. Yeh and Y. L. Liu, A reactive blend of electroactive polymers exhibiting synergistic effects on self-healing and anticorrosion properties, *RSC Adv.*, 2016, **6**, 55593–55598.